



**HAL**  
open science

## Dynamic airspace configuration by genetic algorithm

Marina Sergeeva, Daniel Delahaye, Catherine Mancel, Andrija Vidosavljevic

► **To cite this version:**

Marina Sergeeva, Daniel Delahaye, Catherine Mancel, Andrija Vidosavljevic. Dynamic airspace configuration by genetic algorithm. *Journal of Traffic and Transportation Engineering*, 2017, 4 (3), pp.300 - 314. 10.1016/j.jtte.2017.05.002 . hal-01522033

**HAL Id: hal-01522033**

**<https://enac.hal.science/hal-01522033v1>**

Submitted on 25 Jul 2017

**HAL** is a multi-disciplinary open access archive for the deposit and dissemination of scientific research documents, whether they are published or not. The documents may come from teaching and research institutions in France or abroad, or from public or private research centers.

L'archive ouverte pluridisciplinaire **HAL**, est destinée au dépôt et à la diffusion de documents scientifiques de niveau recherche, publiés ou non, émanant des établissements d'enseignement et de recherche français ou étrangers, des laboratoires publics ou privés.



Distributed under a Creative Commons Attribution - NonCommercial - NoDerivatives 4.0 International License

# Dynamic airspace configuration by genetic algorithm

Marina Sergeeva\*, Daniel Delahaye\*\*, Catherine Mancel, Andrija Vidosavljevic

*Laboratory in Applied Mathematics, Computer Science and Automatics for Air Transport, Ecole Nationale de l'Aviation Civile, Toulouse 31055, France*

## Highlights

- An algorithm to solve a dynamic airspace configuration problem is proposed.
- The considered problem is formulated as a graph partitioning problem and is solved using genetic algorithms.
- Airspace configurations obtained using the developed algorithm, outperform the existing airspace configurations.

## Abstract

With the continuous air traffic growth and limits of resources, there is a need for reducing the congestion of the airspace systems. Nowadays, several projects are launched, aimed at modernizing the global air transportation system and air traffic management. In recent years, special interest has been paid to the solution of the dynamic airspace configuration problem. Airspace sector configurations need to be dynamically adjusted to provide maximum efficiency and flexibility in response to changing weather and traffic conditions. The main objective of this work is to automatically adapt the airspace configurations according to the evolution of traffic. In order to reach this objective, the airspace is considered to be divided into predefined 3D airspace blocks which have to be grouped or ungrouped depending on the traffic situation. The airspace structure is represented as a graph and each airspace configuration is created using a graph partitioning technique. We

optimize airspace configurations using a genetic algorithm. The developed algorithm generates a sequence of sector configurations for one day of operation with the minimized controller workload. The overall methodology is implemented and successfully tested with air traffic data taken for one day and for several different airspace control areas of Europe.

**Keywords:**

Dynamic airspace configuration; genetic algorithm; sectorization

---

\*Corresponding author. Tel.: +33 5 6217 4179.

E-mail addresses: [sergeeva@recherche.enac.fr](mailto:sergeeva@recherche.enac.fr) (M. Sergeeva), [delahaye@recherche.enac.fr](mailto:delahaye@recherche.enac.fr) (D. Delahaye).

## 1 1 Introduction

2 With the continuous air traffic growth and limited resources such as air traffic controllers, there is a need  
3 for decreasing airspace congestion by adapting current airspace design to new traffic demands. In order  
4 to manage air traffic safely and efficiently, the airspace is currently divided into 3D airspace volumes  
5 called *sectors*. An elementary sector is defined as a volume of the airspace within which the air traffic  
6 controller can perform his controlling function. Each sector assigned to a team of controllers is called a  
7 controlled sector. A set of controlled sectors composes an airspace configuration. An air traffic control  
8 (ATC) workload is a way of evaluating an air traffic situation inside the controlled sectors in terms of  
9 several factors. The first factor is related to the number of potential conflicts in the sector. The second  
10 one is linked to the monitoring workload in the sector. The last factor is a coordination workload, which  
11 takes into account all aircraft that cross sector frontiers (in this case pilots and controllers have to  
12 exchange information in order to ensure a safe transfer of aircraft between two sectors).

13 During the course of a day, the ATC workload fluctuates based on traffic demands between various  
14 origin-destination pairings. As the traffic in the airspace is changing with time, it is necessary to consider  
15 dynamic reconfiguration of the airspace for which the number of controlled sectors and their shape will  
16 be adapted to the current traffic situation. Initial sectors can be temporarily combined with others into a  
17 new controlled sector in order to improve efficiency of the airspace configuration. This process is called  
18 dynamic airspace configuration (DAC).

19 In DAC, airspace configurations are generated so as to reduce the coordination workload between  
20 adjacent controlled sectors and to achieve workload balancing between them for each time period of the  
21 day. The DAC process also has to ensure that configurations are stable over time periods. Other  
22 important aspects of DAC concern the reduction of multiple entries of an aircraft in the same sector and  
23 the maximization of the average flight time through the sector. The DAC problem is even more critical in  
24 the SESAR or NextGen framework. In comparison with a currently used fixed route network, the SESAR  
25 program introduces the user preferred routing (UPR) or free routing concept to enable the airspace  
26 users to plan freely 4D trajectories that suit them best. Contrarily to a fixed-route network, a free-route

27 environment will produce a much larger number of different trajectories, for which the dynamic nature  
28 and flexibility of the DAC process will work most efficiently.

29 Our contribution aims at improving today's airspace management in Europe in a pre-tactical  
30 phase. Our research is part of SESAR Programme (Project SJU P07.05.04) co-financed by the EU and  
31 Eurocontrol. The aim of this project is to develop research prototype (decision-support tool) to support  
32 new sectorization methodologies based on 4D trajectories to deal with the implementation of the free  
33 routing concept in the short-term future.

34 In this paper, we present a genetic algorithms (GA) to solve the DAC problem. Our goal is to  
35 produce a solution (airspace configurations for several time periods) that satisfies most constraints and  
36 minimizes all costs. Our approach is based on a graph partitioning algorithm. The method is able to find  
37 a solution even for large problems such as, for example, configuration of the French Airspace for 24 h.

38 This paper is organized as follows: Section 2 presents an overview of related works. In Section 3,  
39 a mathematical model of the DAC problem is proposed. Here, the DAC problem is described as a multi  
40 periods graph partitioning problem. A pre-processing step is presented in this section as well. In Section  
41 4, GA is introduced. Section 5 describes a GA approach for the DAC problem. Results are presented in  
42 Section 6. Finally, conclusions are presented in Section 7.

## 43 **2 Previous related works**

44 Till now, only several works concerning DAC have been produced. In fact, DAC is a quite new paradigm  
45 for airspace systems. The DAC concept consists in allocation of airspace as a resource to meet new  
46 demands of the airspace users. Further introduction to the DAC concept can be found in Kopardekar et  
47 al. (2007) and in Zelinski and Lai (2011). The DAC concept should not be confused with dynamic  
48 sectorization. The main aim of dynamic sectorization is to adapt the airspace to changing needs and  
49 demands of the airspace users, by creating an absolutely new sectorization for each time period of the  
50 day (Chen et al., 2013; Delahaye et al., 1998; Martinez et al., 2007). This means that at each time  
51 period controllers can be obliged to work with new sectors that have different design, as they are not  
52 composed of static airspace blocks, but built from "scratch". From an operational point of view, this is not  
53 desirable, since controllers become more efficient as they become more familiar with airspace, i.e.

54 controlled sectors.

55 Existing approaches on DAC are based on a model in which the airspace is initially divided into 2D  
56 or 3D functional airspace blocks (Delahaye et al., 1995; Klein et al., 2008; Zelinski and Lai, 2011) so that  
57 the DAC problem becomes a combinatorial problem. Configurations are constructed from controlled  
58 sectors, built from pre-defined airspace blocks. Nevertheless, several works are using already existing  
59 and operationally valid ATC sectors (Gianazza, 2010) to construct configurations, or even full  
60 configurations (Vehlac, 2005) to build an opening scheme.

61 Numerous works on airspace configuration have been produced in USA. A comparative  
62 description of 7 works can be found in Zelinski and Lai (2011). In Zelinski and Lai (2011) first three  
63 described works proposed methods for the DAC problem. These works were focused mainly on  
64 reducing delays and reconfiguration complexity in airspace configurations. Among these works, the  
65 most promising one is presented in Bloem and Gupta (2010). This work used as an input a set of given  
66 functional blocks (elementary sectors) and the number of open positions at each period. An output was  
67 a set of controlled sectors grouped into configurations. The workload of the sector was computed as the  
68 maximum number of aircraft in the sector during a given period of time divided by a monitor alert  
69 parameter (MAP). The method minimized a workload cost and a transition cost. It also satisfied several  
70 constraints (taking into account as soft one): bounded workload, connectivity and convexity of controlled  
71 sectors. The uncertainty of trajectory prediction was taken into account as well. The transition cost in  
72 this work was computed as the number of new controlled sectors in the successive configuration. The  
73 model is solved using a rollouts approximate dynamic programming algorithm based on a myopic  
74 heuristic.

75 In Martinez et al. (2007), Chen et al. (2013), Trandac and Duong (2002), Tang et al. (2011),  
76 methods for solving the dynamic sectorization problem (which is related to the DAC problem) were  
77 presented. These works took in consideration most of the important operational constraints. However,  
78 they also contained several weak points from an operational point of view. First, they did not include a  
79 3D design of sectors, including some important airspace design aspects, such as sector shapes. Then,  
80 these approaches did not take into account the stability of the generated configurations in time. In DAC,  
81 generated configurations should have minimal changes from one time period to another, and should be

82 built with operationally workable controlled sectors. As a matter of fact, the more changes between  
83 successive configurations there are, the harder it is for controllers to adapt to a new configuration.  
84 Considering that the duration time of one configuration can be short (the minimum duration time is equal  
85 to 20 min (Eurocontrol, 2015)), too many changes in configurations can induce safety issues.

86 In Klein et al. (2008), instead of using existing sectors, airspace building blocks, called fix posting  
87 areas (FPA), were used. FPAs are assumed to be created in advance. For the complexity metric, rather  
88 than using absolute occupancy counts, a relative metric is computed, i.e., occupancy count (the number  
89 of aircraft in the sector) as a percentage of the sector's MAP value. The dynamic FPA concept is one  
90 form of the flexible airspace management. Sectors are built from FPAs. FPAs can be dynamically  
91 assigned from one sector to other during scheduled sectorization events. In case the sector is  
92 overloaded in a given period of time, algorithm attempts to reassign some of sector's FPAs to a  
93 neighboring sector, if it is possible. If sector is not loaded enough in a given period of time and it has a  
94 neighbor sector whose metric is small enough, then this sector with all its FPAs can be combined with  
95 this neighboring sector. This procedure is repeated for all sectors and all FPAs. The same principle is  
96 used for vertical partitioning of sectors into FPAs, arranged by altitude (e.g., flight levels). In Klein et al.  
97 (2012), the author expanded this concept to create dynamic airspace unit (DAUs). The DAUs are  
98 represented as sector slices near sector boundaries. During pre-defined increments, these units are  
99 dynamically shared between sectors depending on the weather and on the traffic demand. Sector  
100 boundaries adjustments are used in case the complexity metric in one sector is above a certain  
101 threshold.

102 The authors of Gianazza (2010) used existing controlled sectors to create suitable configurations  
103 for different time periods. The decision to reconfigure controlled sectors was driven by the prediction  
104 made by an artificial neural network. A classical tree-search algorithm was used to build all the valid  
105 sector configurations from an initial set of controlled sectors. The tree-search algorithm explored all  
106 possible airspace configurations, among which only one was chosen using evaluation criteria. The  
107 computed configurations were compared to the actual configurations archived by ATC centers.

108 It should be mentioned that most of the existing approaches have been developed for the fixed  
109 airway route network. The main problem of the previous approaches is that they do not include

110 reconfiguration cost. The stability of the generated configurations as well as most important sector  
111 design constraints should be included in the solution of the DAC problem. The next section presents a  
112 model which has been used in our work to address the DAC problem.

### 113 **3 Problem modeling**

#### 114 *3.1 Problem description*

115 Given a forecast on air traffic demand, the DAC problem consists in finding a suitable airspace  
116 configuration for each time period, built from a given set of airspace blocks, such as to minimize some  
117 cost functions. The main objective of the DAC process is to minimize the workload imbalance and the  
118 coordination workload in each airspace configuration. Each configuration should consist of a number of  
119 controlled sectors best suited for the given time period. Controlled sectors should be built from  
120 predefined airspace blocks, such as to be accepted by ATC experts. Therefore, they should satisfy  
121 some geometrical and operational constraints. The quality of the airspace configuration can be  
122 evaluated according to several criteria. In this work, the cost function includes the following criteria.

- 123 • The imbalance between the workload of the resulting controlled sectors.
- 124 • The coordination workload.
- 125 • The number of flight re-entry events.
- 126 • The number of short transits flight through sectors.
- 127 • The number of controlled sectors in each airspace configuration (should not exceed a given  
128 maximum).

129 All those criteria should be minimized during the optimization process. The workload imbalance  
130 minimization means that each sector in each configuration should approximately be loaded with the  
131 same amount of traffic at each period of time. The minimization of the coordination workload, and thus  
132 the controller workload, implies the minimization of the number of traffic flows, cut by sector borders.  
133 Then, the aircraft should not enter the same sector several times. Finally, any entering aircraft must stay  
134 between each sector a given minimum amount of time. This is an important safety constraint, as it  
135 requires a lot of time for the controller to spend on coordination functions. For the controller of the sector,



136 it is hard to manage a conflict between two aircraft in a safe way, if one or both aircraft are passing  
137 through this sector too fast.

138 Then, there are several constraints arising from the sector design methodology. Configurations and  
139 controlled sectors have to satisfy the following constraints.

- 140 • Airspace blocks combined into one controlled sector should be connected.
- 141 • There should be continuity between resulting configurations.
- 142 • Shapes of sectors (in a lateral view) such as "stairs" or "balconies" should be restricted.

143 Last two constraints are considered as soft ones.

144 The presented list of criteria and constraints is designed according to Eurocontrol requirements and  
145 developed in co-operation with operational experts (Eurocontrol, 2015). All those criteria are included in  
146 the model described in the next part.

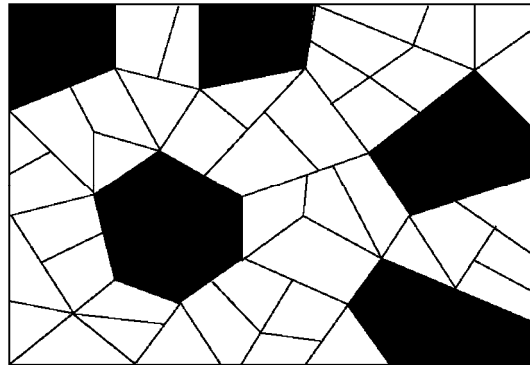
### 147 3.2 *Airspace modeling*

148 According to Kopardekar et al. (2007) and Zelinski and Lai (2011) in the current DAC concept, sector  
149 configurations are constructed by combining existing elementary sectors, provided as an input.  
150 Nevertheless, in this work, we introduce a new DAC concept, proposed and developed in cooperation  
151 with Eurocontrol for SESAR (Eurocontrol, 2015; Sergeeva et al., 2015). This new concept increases  
152 the adaptability of the airspace to the traffic pattern, by delineating from the nominal elementary sectors,  
153 to a larger number of new airspace components, that can be easily combined into rather more adaptable  
154 control sectors. The idea of this concept is that instead of being trained on a full elementary sectors,  
155 airspace controllers can be trained only on a most congested areas, comprised inside smaller airspace  
156 blocks. Two types of airspace blocks are specified in this concept (Fig. 1). In Fig.1, the black blocks are  
157 non-sharable and the white ones are sharable.

158 (1) Sector building blocks (SBBs) are permanently busy areas with a high traffic load, delineated by  
159 recurring traffic patterns. Often, SBBs blocks are small and cannot be sub-divided further. Each SBB is  
160 considered as a core of a future control sector. SBBs can be sufficiently large than SAMs, in order to be  
161 workable and controllable. It should be noticed that the control sector should include at least one SBB.

162 (2) Sharable airspace modules (SAMs) are built in less busy areas with a temporary high traffic

163 load. SAMs can be re-allocated laterally or vertically between neighboring control sectors within a sector  
164 configuration process, in order to equally balance the traffic load among the control sectors. SAMs  
165 cannot be used separately in the configuration.



166  
167 **Fig. 1** Initial airspace blocks (2D projection).

168 Each controlled sector is supposed to be built of at least one non-sharable block and several  
169 sharable blocks. Building of the controlled sector starts from choosing a central block, which can be  
170 chosen only among non-sharable blocks. The number of non-sharable blocks is limited; this guarantees  
171 that the central part of each controlled sector will be stable between several configurations. Even if the  
172 number of controlled sectors is different in two successive configurations, centers of the controlled  
173 sectors will be chosen among the same small group of non-sharable blocks. This partly insures  
174 continuity between successive airspace configurations.

### 175 3.3 Graph modeling

176 In this section we describe a weighted graph model of the airspace. Let a graph  $G = (N, L)$  represent the  
177 airspace, where  $N$  is a set of nodes and  $L$  is a set of links. In this graph each node represents sharable  
178 or non-sharable block and each link represents the relation is neighbor with between two nodes (Fig. 2),  
179 it means that when two blocks share a common vertical or horizontal border, a link is built between  
180 them. In Fig.2, solid nodes represent non-sharable blocks, and hollow nodes represent sharable blocks.  
181 Weight of the node represents the monitoring workload and weight of the link represents the  
182 coordination workload.

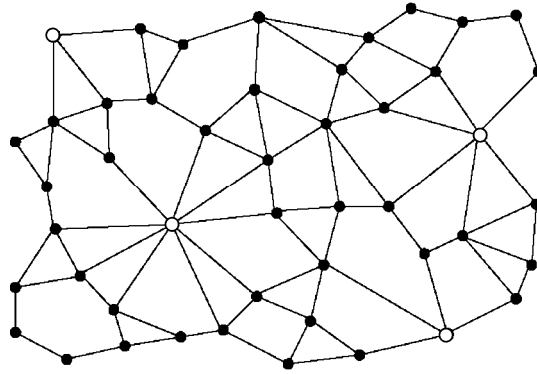


Fig. 2 Example of the initial graph.

183

184

185 The workload assessment is a key requirement for generation of the workable sector  
 186 configurations in a context of free route environment. In order to evaluate the monitoring workload, in  
 187 each block, an occupancy count is used. The occupancy count metric is computed as the number of  
 188 aircraft inside the airspace block at each minute of an associated time period. The weight of the link  
 189 (coordination workload) is computed as the number of aircraft crossing the border between two airspace  
 190 blocks connected by this link. Both monitoring and coordination workloads of airspace blocks are  
 191 computed for each given time period.

### 192 3.3 A graph partitioning problem

193 Based on the weighted graph described above, our problem consists in finding an optimal multi-period  
 194 graph partitioning. For each given time period, we must find an optimal grouping of airspace blocks that  
 195 satisfies all the constraints. The time periods (opening scheme) are considered to be an input data.

196 A connectivity constraint on airspace blocks belonging to the same sector means that nodes  
 197 belonging to the same component have to be connected. This means that for each pair of nodes  
 198 belonging to the same component, there is a path connecting them.

199 For a given time period  $t_i$ , the resulting configuration is modeled in the following way:  $X_i = \{N_1,$   
 200  $N_2, \dots, N_{K_i}\}$ , where  $N_j$  represents the set of nodes belonging to the component  $j$ ,  $K_i$  represents here the  
 201 number of component for time period  $t_i$ .  $K_i$  value is controlled by the optimization process and has to be  
 202 less than  $S_n$ , where  $S_n$  is the maximum number of available controllers. Having a problem with several  
 203 time periods  $\{t_1, t_2, \dots, t_p\}$ , the associated graph partitioning problem have to be optimized for each

204 period.

$$205 \quad \begin{cases} X_1 = \{N_{11}, N_{12}, \dots, N_{1K_1}\} & \text{for } t_1, K_1 \\ X_2 = \{N_{21}, N_{22}, \dots, N_{2K_2}\} & \text{for } t_2, K_2 \\ \vdots \\ X_P = \{N_{P1}, N_{P2}, \dots, N_{PK_P}\} & \text{for } t_P, K_P \end{cases} \quad (1)$$

### 206 3.3 Objective function

207 Based on the state space definition, we now model the associated objective function. Five criteria are  
208 included in our objective function for evaluation of a solution (resulting configurations).

209 The first criterion measures the total level of the workload imbalance in each configuration,  
210 separately for each time period  $t_i$  ( $i = 1, 2, \dots, T$ ). The workload of the controlled sector is computed as a  
211 sum of the workloads of airspace blocks which are composing this sector. The workload imbalance of all  
212 sectors in the configuration for the time period  $t_i$  is computed using Eq. (2).

$$213 \quad U_t = \sqrt{\frac{\sum_{k=1}^{K_i} \left( \frac{\|W_{c_{ik}} - c\|}{c} \right)^2}{k_i}} \quad (2)$$

214

215 where  $K_i$  is the number of controlled sectors in the configuration for period  $t_i$ ,  $W_{c_{ik}}$  is the total workload of  
216 all airspace blocks composing the sector  $k$  for period  $t_i$ ,  $c$  is a targeted workload of the sector.

217  $c$  is a user-defined parameter and can be computed, for example, as a capacity of a sector. The  
218 capacity of a controlled sector can be defined as the maximum number of aircraft that are controlled in a  
219 particular sector in a specified period, while still permitting an acceptable level of controller workload  
220 (Majumdar and Ochieng, 2002). The way sector capacity is computed depends on the controller  
221 workload definition. Often it is computed as the maximum number of flights that a controller can handle  
222 in one hour without breaking a theoretical threshold (Christien et al., 2003). In this work, the  
223 maximum sector capacity is taken for 1 min (the workload is computed as occupancy count). The  
224 maximum acceptable number of flights per 1 min is equal to 8 (this number was provided by

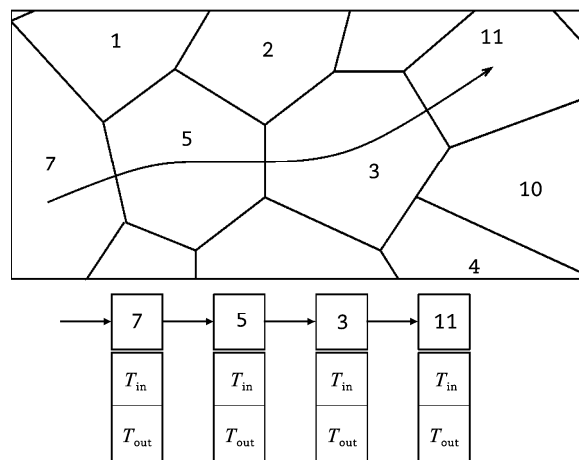
225 Eurocontrol and reflects realistic operational value). Then, the maximum sector capacity for the  
 226 time period of 1 h is equal to 8 aircraft multiplied by 60 min. As we would like to obtain controlled  
 227 sectors that are not extremely loaded,  $c$  is computed as the maximum sector capacity weighted by the  
 228 reduction coefficient, which is equal to 75% (value provided by Eurocontrol). Then, for the time period of  
 229 1 h, the targeted workload  $c$  is equal to 360.

230 The second criterion included in the objective function, measures the transfer traffic between  
 231 neighboring blocks (a flow cut). When two neighboring blocks belong to different sectors, the traffic flow  
 232 between them is getting cut by the sector's border, increasing the coordination workload of sectors. The  
 233 total flow cut for the time period  $t$  ( $FC_t$ ) is given by Eq. (3).

$$234 \quad FC_t = \sum_{\substack{(i,j) \in L \\ i \in N_m, j \in N_m \\ m \neq n}} f_{ij}^t + f_{ji}^t \quad (3)$$

235 where  $f_{ij}^t + f_{ji}^t$  is the number of aircraft crossing the border between blocks  $i$  and  $j$  (in both directions) at  
 236 the time period  $t$ , computed using a known set of links.

237 The number of re-entries ( $N_{r_t}$ ) and the number of short transits ( $N_{s_t}$ ) inside the controlled sectors at  
 238 the time period  $t_i$  are included in the objective function as well. In order to be able to compute re-entry  
 239 events and short transits inside created controlled sectors, we register the list of airspace blocks  
 240 crossed by each trajectory with the associated time horizon (Fig. 3). In Fig.3, each element of a list  
 241 contains the ID of a block and a crossing time.



242  
 243 **Fig. 3** List of airspace blocks associated to a given trajectory.  
 244 Then, using this list of airspace blocks associated to each trajectory (list of traversed blocks), it is

245 possible to compute  $N_{r_t}$  and  $N_{s_t}$  for each time period. It is done in several steps.

246 (1) We first transform a list of associated airspace blocks into a list of controlled sectors associated to  
247 each trajectory.

248 (2) To compute the re-entries, we check if in the aircraft's list of traversed sectors there is no situation  
249 when the aircraft enters the same sector several times, and if there is, we add one re-entry to  $N_{r_t}$ .

250 (3) For computing the number of short-crossings, we check the time that the aircraft stays in each  
251 sector, and if this time is smaller than a given value, we add one short-crossing to  $N_{s_t}$ .

252 Finally, the last criterion included in our objective function ( $N_{b_t}$ ) measures the number of "balconies".  
253 This type of sector shape (in the lateral view) is not desirable but acceptable, that is why this criterion is  
254 included in the objective function. The number of "balconies" is computed during the evaluation process,  
255 using the set of links.

256 All those criteria are normalized in order to have values  $\in (0, 1)$  and aggregated into one objective  
257 function (Eq. (4)) which is used to evaluate each configuration, created during the optimization process.

$$258 \quad \min(y) = \alpha_1 U_t + \alpha_2 Fc_t + \alpha_3 N_{r_t} + \alpha_4 N_{s_t} + \alpha_5 N_{b_t} \quad (4)$$

259 where  $\alpha_1 - \alpha_5 \in (0, 1)$  are proportion coefficients.

260 Then, the objective function associated to the whole planning is computed as an average value of  
261 the evaluation of each configuration. The proportion coefficients in the objective function enable to  
262 obtain optimized results for different scenarios.

263 The number of the controlled sectors in configuration is minimized during the optimization process,  
264 due to minimization of the workload imbalance (while trying to keep sectors workload close to a given  
265 value, we also optimize the number of sectors in each configuration).

### 266 3.4 Combinatorial optimization problem

267 Based on the airspace model described above, the DAC problem is formulated as a combinatorial  
268 optimization problem, which consists in finding an optimal partitioning of the graph into several  
269 connected sub-graphs for each defined time period. Moreover, several operational constraints have to  
270 be taken into account during the partitioning process and this makes it difficult to use most common

271 techniques for solving the graph partitioning problem.

272 The proposed formulation of the DAC problem, as a graph partition problem, is highly combinatorial.

273 The size of the state space (the number of states that the problem can be in) depends on the number of

274 blocks  $N_b$ , on the number of controlled sectors  $K_i$  and on the number of opening time periods  $N_t$ . For

275 each time period we must find an optimal grouping among  $S_{N_b}^{K_i}$  of possible combinations of  $N_b$  blocks

276 into  $K_i$  sectors, where  $S_{N_b}^{K_i}$  is a second Stirling number. The second Stirling number is computed using

277 Eq. (5).

$$278 \quad S_{N_b}^{K_i} = \frac{1}{K_i!} \sum_{j=0}^{j=K_i-1} (-1)^j \left( \frac{K_i!}{j!(K_i-j)!} \right) (K_i-j)_b^N \quad (5)$$

279

280 The state space of our problem is discrete and its size grows exponentially fast. An example of the

281 number of possible combinations of 16 blocks is shown below.

$K_i$	$S_{16}^{K_i}$	$K_i$	$S_{16}^{K_i}$
1	1	9	820,784,250
2	32,767	10	193,754,990
3	7,141,686	11	28,936,908
4	171,798,901	12	2,757,118
5	1,096,190,550	13	165,620
6	2,147,483,647	14	6020
7	2,147,483,647	15	120
8	2,141,764,053	16	1

282

283 The combinatorics of such a problem can become extremely high, especially if we want, for

284 example, to obtain airspace configurations for the whole day and we take one time period equal to 30

285 min.

286 Typically, graph partition problems fall under the category of NP-hard problems (for more details

287 see Kernighan and Lin (1970), Savage and Wloka (1989)). For an NP-hard problem, where

288 state-of-the-art exact algorithms cannot solve the handled instances within the required search time, the  
289 use of metaheuristics is justified. Metaheuristics do not guarantee to find optimal solutions, however,  
290 they allow to obtain good solutions in a significantly reduced amount of time (Blum and Roli, 2003; Talbi,  
291 2009). Their use in many applications shows their efficiency in solving large NP-hard problems.  
292 Metaheuristics can be roughly divided into population-based algorithms and non-population-based  
293 algorithms (Talbi, 2009). While solving optimization problems, non-population-based metaheuristics  
294 improve only one solution, while the population-based algorithms explore the search space by evolving  
295 a whole population of candidate solutions. Population-based metaheuristic methods are well adapted  
296 for problems that require not a lot of memory to code the state space (in our case, it requires less than 1  
297 Mb).

298 The proposed model of DAC can be solved using different techniques (Antosiewicz et al., 2013;  
299 Han and Zhang, 2004; Silberholz and Golden, 2010). Non-population-based algorithms, such as  
300 Simulated Annealing for example, can allow to converge more rapidly to an optimal solution than  
301 population-based algorithms (Kohonen, 1999). Nevertheless, the convergence speed mainly depends  
302 on the implementation of the algorithm and on the size of the state space of the problem. In case of the  
303 problem with a large state space of feasible solutions (like the DAC problem), it is hard to avoid  
304 non-population-based algorithms getting stuck at local minima. On the other hand, in population-based  
305 algorithms, solutions are being independently improved at the same time and this makes this type of  
306 algorithms less prone to get stuck in local optima than alternative methods (Mukherjee et al., 2015; Nair  
307 and Sooda, 2010; Rossi-Doria et al., 2002).

308 The DAC problem can have several different optimal solutions, due to the different possible  
309 symmetries in the topological space. As we have several objectives to be satisfied, we can obtain  
310 several different solutions with the same value of the objective function. We must be able to find most of  
311 the near-optimal solutions, as they have to be evaluated and refined by experts. This last point makes  
312 us reject non-population-based algorithms which update only one state variable, i.e. improve only one  
313 possible solution.

314 In this work, we aim to obtain a compromise between the quality of the solution and the CPU time  
315 required to reach it. Population-based algorithms, such as EAs, maintain and improve a population of



316 numerous state variables according to their fitness and are able to find several optimal solutions. EAs  
317 can guarantee stable optimization results even for big problem instances, computed within a reasonable  
318 time. EAs are also a good choice if we would like to extend our model to a multi-objective one. Thus,  
319 EAs are relevant to solve the DAC problem.

#### 320 **4 Evolutionary algorithms**

321 Evolutionary algorithms (Back et al., 1991; Davis, 1991; Fogel and Owens, 1966; Goldberg, 1989;  
322 Holland, 1975; Koza, 1992; Michalewicz, 1992) use techniques inspired by evolutionary biology to find  
323 approximate solutions of optimization problems. An individual, or solution of the problem, is represented  
324 by a list of parameters, called chromosome. Initially several such individuals are randomly generated to  
325 form the first initial population ( $POP(k)$  in Fig. 4). Then each individual is evaluated, and a value of fitness  
326 is returned by a fitness function. This initial population undergoes a selection process which identifies  
327 the most adapted individual. The one which is used in our work is a deterministic  $(\lambda, \mu)$ -tournament  
328 selection (Miller and Goldberg, 1995). This selection begins by randomly selecting  $\lambda$  individuals from the  
329 current population and keep the  $\mu$  best ( $\lambda > \mu$ ). These two steps are repeated until a new intermediate  
330 population ( $POP_i$ ) is completed. Then, three following recombination operators are applied to individuals:  
331 nothing ( $1 - P_c - P_m$ ), crossover ( $P_c$ ), or mutation ( $P_m$ ) with the associated probability respectively.

332 The chromosomes of two parents are mixed during crossover resulting in two new child  
333 chromosomes, which are added to the next population. Mutation is an operator used to maintain genetic  
334 diversity from one population of chromosomes to the next one. The purpose of mutation in EAs is to  
335 allow the algorithm to avoid local minima by preventing the population of chromosomes from becoming  
336 too similar to each other, thus slowing or even stopping evolution.

337 These processes ultimately result in the next population of chromosomes ( $POP(k+1)$  in Fig. 4). This  
338 process is repeated until a termination condition has been reached. As a termination condition, we can  
339 use the maximum number of generations. In Fig.4, on the first step best individuals are selected from  
340 population  $POP(k)$ . Then, recombination operators are applied to produce the  $POP(k+1)$  population.

341

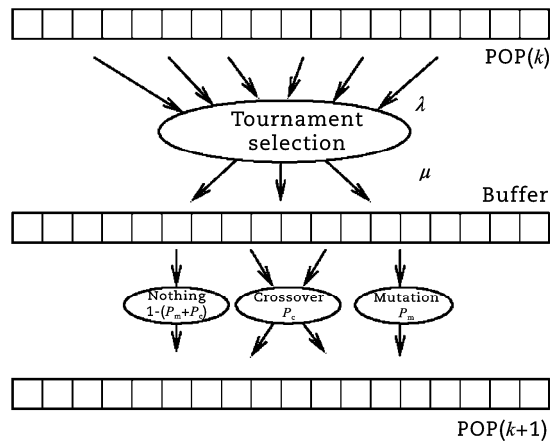


Fig. 4 Genetic Algorithm with tournament selection.

342

343

344

## 345 5 Application of GA to the DAC problem

### 346 5.1 Coding the chromosome

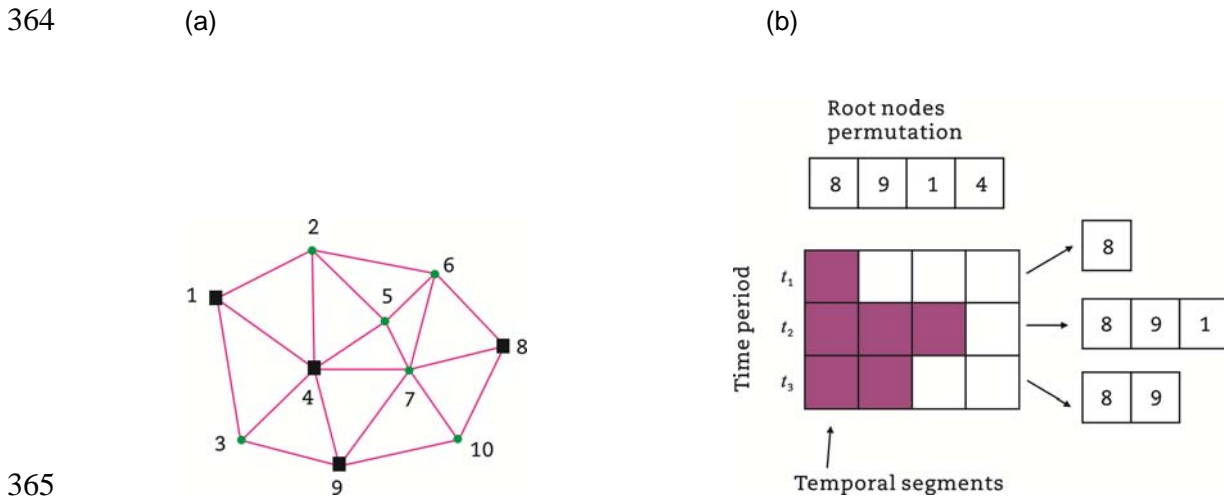
347 Based on the proposed problem modeling, a way of coding configurations for each time period  
 348 (chromosome) has to be developed. In the previous section, we have proposed a way of modeling the  
 349 airspace configuration as a set of connected components (subgraphs). The coding used for this problem  
 350 consists in representing connected components by sub-sets of nodes for each time period.

351 The chromosome used in this work consists of two layers. The first layer controls the number of  
 352 opened controlled sectors and theirs centers per each time period. The second layer contains all  
 353 sub-sets of connected components obtained for each time period, i.e., the list of all airspace blocks with  
 354 the associated number of the controlled sector for each time period. Thus, the first layer controls root  
 355 nodes (non-sharable blocks) and consists of two tables. The first table includes all permuted  
 356 non-sharable nodes and the second one contains temporal segments for each root node (Fig. 5). In Fig.  
 357 5, non-sharable blocks (potential root nodes) are represented as squares and sharable blocks as  
 358 circles.

359

360 The temporal segments include the information about the number of the controlled sectors used per

361 each time period. The second layer manages the set of connected components (for each time period)  
 362 and is represented as a table that contains all nodes with their associated component number (Section  
 363 5.2).

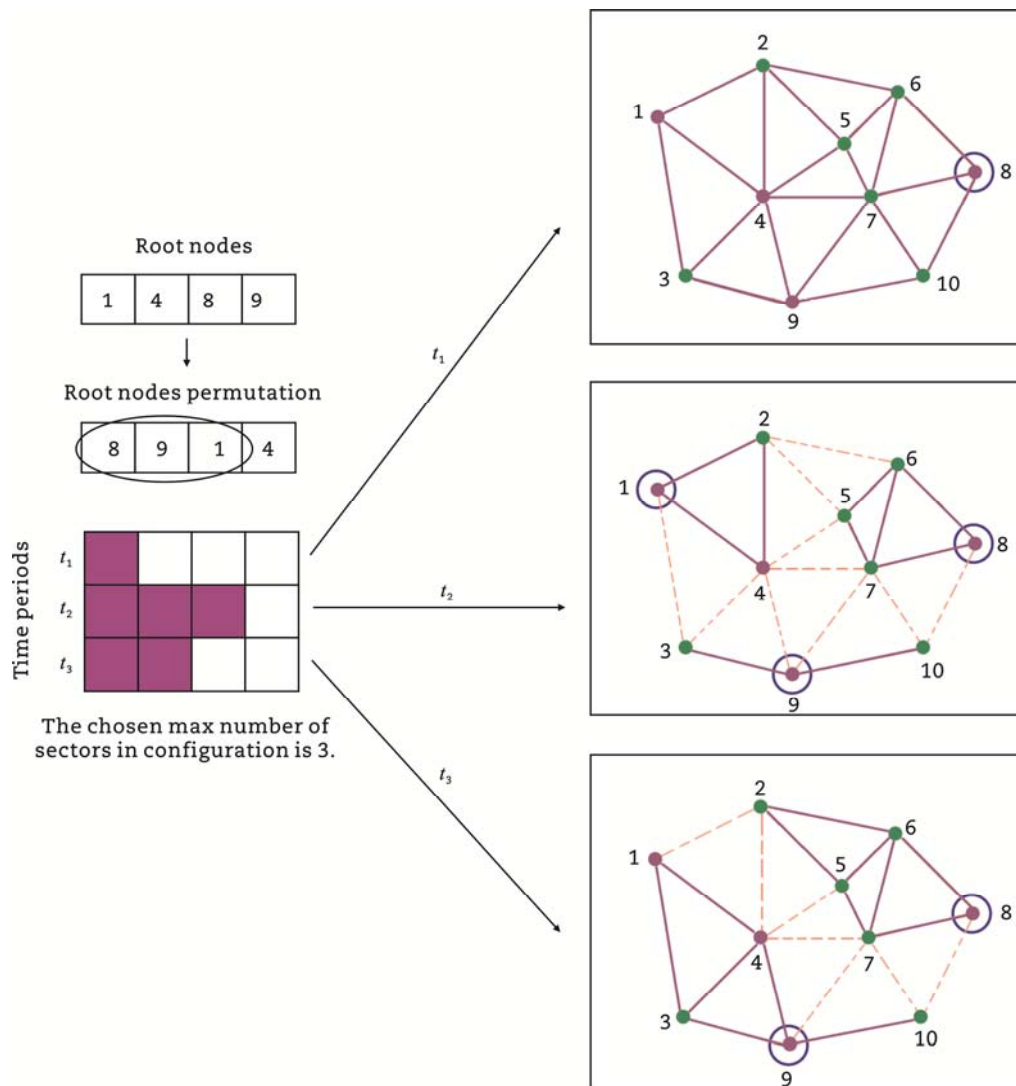


365  
 366

**Fig. 5** Chromosome structure. (a) Initial graph. (b) First layer of chromosome.

367 **5.2 Initialization of the chromosome**

368 Each solution (chromosome) in a population is first initialized randomly. As our chromosome consists of  
 369 two parts, the process of initialization of the chromosome is divided into two steps. On the initial step, for  
 370 each time period, several root nodes are randomly selected from the permutation table (initially this  
 371 table is randomly generated for each solution in the population) which contains all non-sharable nodes  
 372 as shown in Figs. 5 and 6. Those selected nodes are considered as root nodes - central parts of each  
 373 subgraph. The minimum number of root nodes that can be selected is equal to 1 and the maximum is  
 374 equal to the maximum allowed number of the controlled sectors per configuration, i.e., to the number of  
 375 available controllers.



376

377 **Fig. 6** Resulting graph partition for the 3 time periods, obtained using a table of root nodes and temporal time segments.

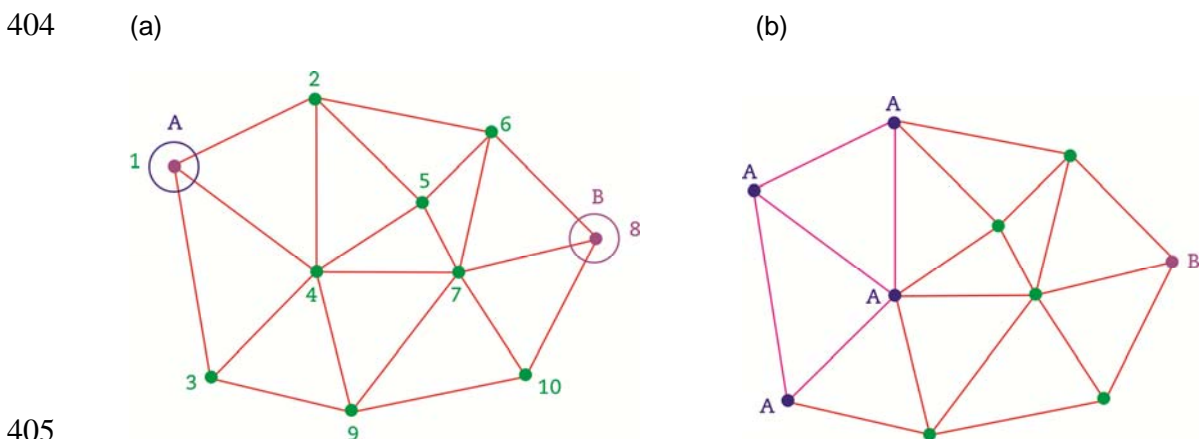
378 On the next step, temporal segments are randomly built. After this, all selected root nodes are  
 379 associated with time periods. For each time period, several root nodes can be selected. The number of  
 380 the selected root nodes per time period is first chosen randomly and then is optimized in the algorithm.  
 381 The first root node in the permutation table participates in the partitioning process for each time period  
 382 (node 8 in Fig. 6).

383 In the example illustrated in Fig. 6, the number of non-sharable nodes and potential root nodes is  
 384 equal to 4 (nodes 1, 4, 8 and 9) and the maximum number of the controlled sectors per configuration is  
 385 equal to 3. Three time periods are considered and three temporal time segments are generated  
 386 randomly. Each time segment cannot have a length bigger than 3. At the time period 1 there is one

387 sub-set created with root node 8, and time period 2, with root nodes 8, 9 and 1, and etc. The initial  
 388 permutation of the root nodes in different solutions ensures a random mapping between temporal  
 389 segments and root nodes (this avoids the same root node to be associated with the first temporal  
 390 segment in different solutions).

391 This way of coding the chromosomes with temporal segments ensures the stability in time of  
 392 shapes of controlled sectors. For successive time periods, the same root nodes are used as sector  
 393 centers, ensuring these volumes of airspace being controlled by the same controllers. As a matter of  
 394 fact, compared with the other works on DAC, the main advantage of our method is that the stability of  
 395 configurations in time is insured by the proposed model of the configuration process. Most of the  
 396 existing methods in the literature, instead, include a reconfiguration cost as one of the objectives. This  
 397 cannot always insure the stability of configurations in time, as often the reconfiguration cost is computed  
 398 simply as a difference of the number of the controlled sectors in the successive configurations.

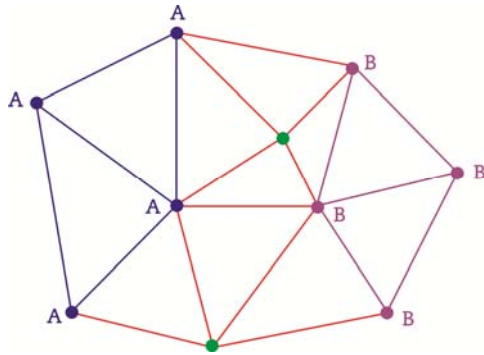
399 After producing the first layer of the chromosome, a graph partitioning algorithm is applied for the  
 400 second layer. In the example illustrated in Fig. 6, for 3 time periods, 3 subgraphs are built, using the  
 401 associated list of selected root nodes for each time period. The developed graph partitioning algorithm  
 402 ensures that nodes of the same sub-set are connected by at least one path. The process of building  
 403 connected components using greedy heuristic is illustrated in Fig. 7.



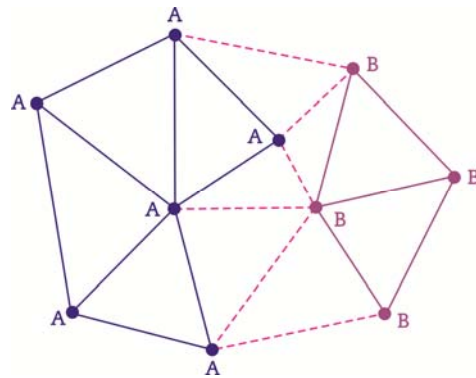
405  
 406  
 407  
 408

409

(c)



(d)



410

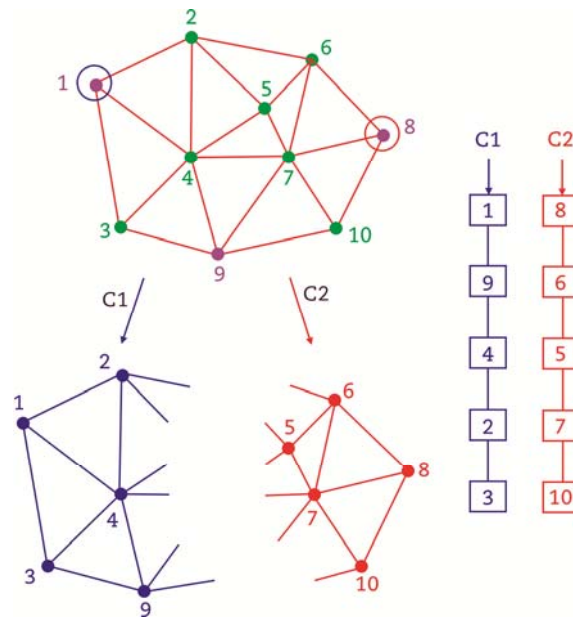
411

**Fig. 7** Greedy heuristic is used to create initial partitions. (a) Step 1. (b) Step 2. (c) Step 3. (d) Step 4.

412

This heuristic takes the first root node and propagates it on its neighbours (step 2). Then, the second root node is propagated also on its neighbours (step 3). Then, the algorithm propagates again the first component (step 4) and this process is repeated until all nodes are associated with their components. At the end, each connected component is coded as a list of nodes (Fig. 8).

415



416

417

**Fig. 8** Example of the coding used for one time period. Here, the graph is partitioned into two components using two root nodes 1 and 8.

418

419

After creating the first population of solutions, each solution is evaluated using the objective function. Then, after the selection process, the recombination operators are applied resulting in a new population.

421

422 5.3 *Recombination operators*

423 5.3.1 *Recombination operators for the first layer of the chromosome*

424 The first layer of the chromosome controls the choice of root nodes used for all time periods.

425 (1) Temporal segment crossover

426 In this crossover operator, two or more solutions (parents) exchange part of their chromosome,  
427 resulting in two new solutions. Based on time interval sets from two randomly selected solutions, a  
428 crossover has been developed in which, most probably, the individual with the worst performance will  
429 receive temporary segments of the second one (i.e., we copy the first layer of chromosome from a good  
430 solution to a bad one).

431 (2) Temporal segment mutation

432 The mutation operator starts by selecting a solution from the population. An individual with low  
433 performances has more chances to be selected. Then one configuration is selected either randomly or  
434 according to its performance. This mutation operator changes the number of the temporal segments in  
435 the solution by adding or removing one segment, i.e., adding or removing one controlled sector into  
436 configuration for a selected time period. The number of segments has to stay in the following range  $[1,$   
437  $|N_R|]$  where  $N_R$  is the set of root nodes in the network.

438 (3) Root nodes mutation

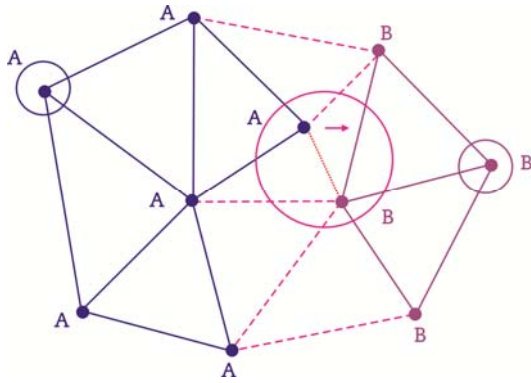
439 The mutation operator starts with randomly selecting a solution from the population. The aim of  
440 this operator is to change initial permutation table of root nodes. The operator simply changes the order  
441 of root nodes by randomly exchanging two nodes in the permutation table.

442 5.3.2 *Recombination operators for the second layer of the chromosome*

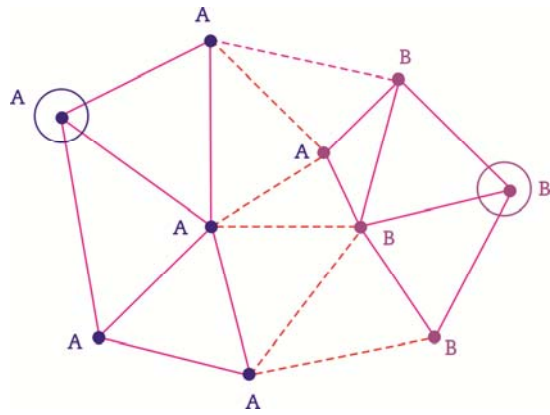
443 For the second layer, we only use one mutation operator. After choosing a solution from the population,  
444 the operator selects a time period according to the associated graph partitioning performances,  
445 meaning that a bias is added for the period with a low performance. Then the graph partitioning mutation  
446 operator is applied (Fig. 9).

447

448 (a)



(b)



449

450 **Fig. 9** Graph partitioning results for the second layer of the chromosome. (a) Before applying the developed mutation operator.

451 (b) After applying the developed mutation operator.

452 This operator begins by statistically selecting the component with the worst performance. Then, in  
453 case the selected component is overloaded (sector workload > targeted workload), it seeks the  
454 neighbouring component with the least load. In case the selected component is underloaded, the  
455 operator searches the neighbouring component with the higher load. This second step is also carried  
456 out statistically (introducing a bias into a random selection). We thus obtain a link between the two  
457 components. A node is then moved from the most loaded component to the least loaded one, while  
458 verifying that the component losing a node remains connected.

## 459 6 Results and discussions

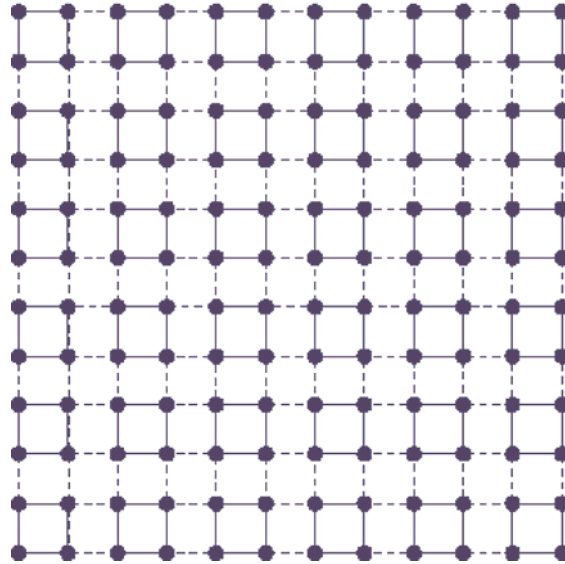
460 This algorithm has been tested on several different problems in order to check its efficiency and its  
461 future perspective. The algorithm is able to provide different kind of results according to expert  
462 requirements.

### 463 6.1 First test: application to a network with symmetries

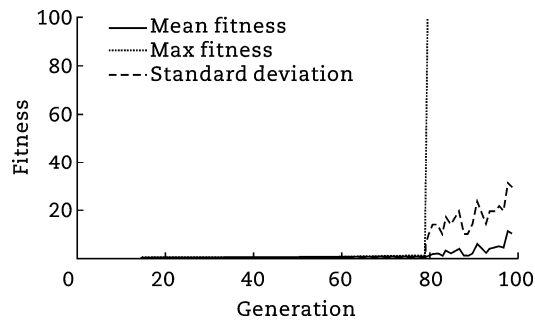
464 In order to evaluate this algorithm, a network with symmetry has been built for which, a solution is easy  
465 to investigate for a human being due to our ability to see such symmetry but which has no particular  
466 features for the algorithm. This network is built with 144 blocks which are extended on 10 time periods.  
467 Those 144 blocks are symbolized by nodes on the graph in Fig. 10. For this network it is very easy to



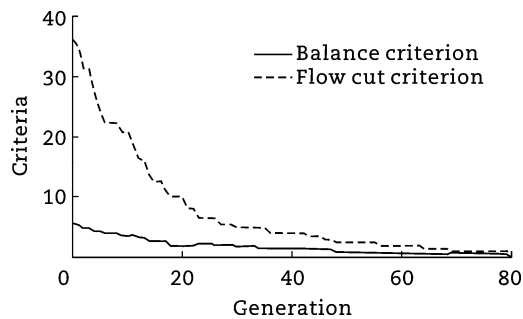
468 identify 36 sectors. With only 100 individual in the population and 100 generation, the algorithm is able  
469 to identify the best solution at generation 80 as it can be seen on Figs. 11 and 12.



470  
471 **Fig. 10** Graph with symmetries.  
472



473  
474 **Fig.11** Graph with symmetries: fitness evolution (mean, max, standard).



475  
476 **Fig. 12** Graph with symmetries: criteria evolution (balance, flow cut).  
477

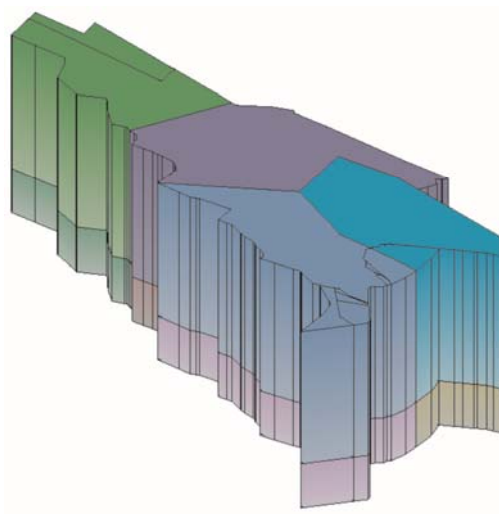
478 Having validated our algorithm on the toy network, we propose now to apply it on a real airspace.

479

## 480 6.2 Second test: application to a real airspace

481 Our algorithm has been tested on a Maastricht (EDYYBUTA) Area Control Center (ACC). This area  
482 initially consists of 8 elementary sectors. For this second test we have prepared two scenarios. In the  
483 first scenario, we use existing elementary sectors of today's airspace (Fig. 13). Those sectors are big  
484 and not flexible enough, as they are loaded differently during the day. For this scenario, the number of  
485 initial sectors is small, and so all of them are considered as non-sharable blocks. In the second scenario,  
486 we use 32 sharable and non-sharable blocks (Fig. 14) located on 2 altitude layers and created only for  
487 the purpose of our experiments in order to increase the flexibility of new sector configurations (Sergeeva  
488 et al., 2015). These blocks are much smaller; as a result, the workload is better distributed between  
489 them. Each scenario is based on free route simulated trajectories, which provide a sample of full free  
490 route trajectories for the 11th of July 2014 crossing Maastricht/Amsterdam Airspace.

491 Tuning of the controlling parameters of the algorithm (such as generations number, population size,  
492 mutation/crossover ratio) is required due to the specific properties of each airspace area. The parameter  
493 values are selected after running several tests in order to obtain a required result.



494

495

**Fig. 13** Eight elementary sectors of the Maastricht ACC (EDYYBUTA).

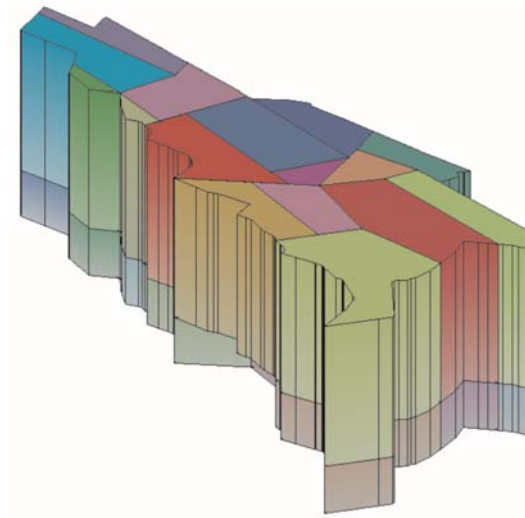


**Fig. 14** Thirty-two experimental sharable and non-sharable blocks.

496

497

498

499

500 In this test, the mutation rate is selected to be bigger than the crossover rate, as the mutation  
501 operators allow the algorithm to converge faster. The number of generations and the size of the  
502 population are chosen according to the size of the network. For example, the first scenario requires  
503 smaller number of generations in order to obtain a near optimum solution. The values of proportion  
504 coefficients in the objective function are chosen according to interviewed operational experts. The  
505 highest priority is given the workload imbalance minimization. The remaining criteria are sorted by  
506 priority as follows: short-crossings, re-entries, the number of “balconies” and flow cuts.

507 The parameters defining the overall resolution methodology for both scenarios are empirically set,  
508 and presented in Table 1.

509 Numerical results from computational experiments for two proposed scenarios are presented in  
510 Tables 2 and 3. These two tables include the following data (per each time period): the number of  
511 sectors in the configuration, an average workload imbalance per 1 h, the number of re-entries and the  
512 number of short-crossings. The execution time for both scenarios is less than a few minutes (1-2 min).

513

514

515

516

**Table 1** Values of main criteria of the algorithm.

Parameter	Scenario 1	Scenario 2
Generations	200	1000
Population size	300	1000
Mutation/crossover ratio	0.6/0.2	0.6/0.2
Targeted workload	360	360
Time period (h)	7 – 18	7 – 18
Period size (h)	1	1
$\alpha_1, \alpha_2, \alpha_3, \alpha_4, \alpha_5$	0.6, 0.05, 0.1, 0.1, 0.2	0.6, 0.05, 0.1, 0.1, 0.2

517

**Table 2** Results for the scenario 1.

Time period (h)	Number of sectors	Imbalance	Number of re-entries	Number of short-crossings
7 – 8	4	0.10	0	1
8 - 9	5	0.24	0	6
9 – 10	5	0.30	0	11
10 – 11	5	0.22	0	7
11 - 12	5	0.19	0	9
12 – 13	4	0.20	0	3
13 – 16	6	0.18	0	9
16 – 17	4	0.24	0	8
17 – 18	4	0.10	0	6

518

**Table 3** Results for the scenario 2.

Time period (h)	Number of sectors	Imbalance	Number of re-entries	Number of short-crossings
7 – 8	5	0.10	4	7
8 – 9	5	0.14	3	11
9 – 10	5	0.18	2	6
10 – 11	5	0.17	7	8
11 – 12	5	0.13	2	8
12 – 13	5	0.12	5	8
13 – 14	6	0.14	4	8
14 – 15	6	0.08	6	8
15 – 16	5	0.05	2	9
16 – 17	5	0.08	1	5
17 – 18	4	0.06	2	6

519

520 Controlled sectors built by the algorithm for the second scenario are much better balanced in  
 521 terms of the workload than sectors built for the first scenario. However, some of the sectors proposed for  
 522 the second scenario have undesired shapes like “balconies”. Nevertheless, balanced sectors with only  
 523 few “balconies” are considered by operational specialists as an acceptable solution. Then, the number  
 524 of re-entries is higher for the second scenario, this is explained by the shape of the initial blocks; they do  
 525 not have enough convex shapes, thus, combinations of such blocks are not well adapted to a traffic  
 526 pattern.

527 The second scenario proves the idea of using more adaptive blocks instead of those that are  
 528 currently used in the airspace management. As a matter of fact, the quality of the workload balance is  
 529 mainly linked to the number of input blocks. With a bigger number of input blocks we can obtain less  
 530 unbalanced sector configurations.

531 From the provided results we can conclude that the algorithm is quite efficient for the workload  
 532 balancing. However, it is hard for the algorithm to remove all defects of sector shapes such as  
 533 “balconies” and obtain sectors with convex shapes. The algorithm can later be modified in order to  
 534 receive rather convex shapes of the resulting sectors in both horizontal and vertical directions.

535 Next we compare configurations built by the algorithm with the existing configurations (Table 4),  
 536 used at the day of operation and also with the solution built by the improved configuration optimizer (ICO)  
 537 system tool (Table 5) of Eurocontrol (Vehlac, 2005). The ICO tool uses a limited number of predefined  
 538 sectors configurations to construct a full timetable for the day (an opening scheme), based on known  
 539 traffic pattern and current organizational framework. ICO provides a limited flexibility, as it uses already  
 540 existing configurations that are not well adapted to the traffic. In order to evaluate the workload  
 541 imbalance in those configurations, instead of using the same targeted workload as in two solution  
 542 scenarios, we use an average workload of sectors in each configuration.

543 **Table 4** Evaluation of existing configurations.

Period	Number of sectors	Imbalance	Number of re-entries	Number of short-crossings
06:30 - 08:00	5	0.37	1	10
08:00 - 09:30	6	0.36	0	15
09:30 - 11:00	5	0.33	0	20

11:00 - 12:00	6	0.42	2	14
12:00 - 13:30	5	0.38	0	20
13:30 - 14:30	6	0.48	0	12
14:30 - 15:00	5	0.35	0	3
15:00 - 15:30	6	0.43	0	4
15:30 - 18:00	5	0.19	2	20

544

545

**Table 5** Evaluation of the ICO tool results.

Period	Number of sectors	Imbalance	Number of re-entries	Number of short-crossings
07:11 - 08:10	6	0.28	0	6
08:11 - 09:10	6	0.31	0	6
09:11 - 10:49	6	0.34	0	22
10:50 - 12:06	6	0.39	2	21
12:07 - 14:02	6	0.39	0	15
14:03 - 15:02	6	0.36	1	10
15:03 - 16:43	6	0.30	1	21
16:44 - 18:15	6	0.26	1	18

546

547

548

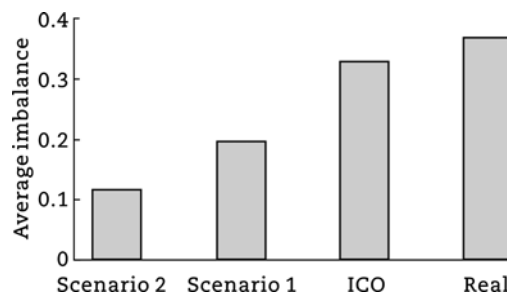
549

550

551

552

Fig. 15 shows a significant improvement of the quality of the configurations provided by the solution scenarios, especially in terms of the workload balancing. The results of the ICO tool show worse performance, as this tool does not improve configurations, but it selects for each computed time period one suitable configuration among the existing ones. In the future research, the output of our algorithm can be used as an input for the ICO tool, and a combination of both algorithms could provide better results.



553

554

555

**Fig. 15** An average workload imbalance in configurations proposed by the algorithm (for two scenarios), in existing configurations and in configurations proposed by the ICO tool.

556 It can be seen that configurations from Tables 2, 3, 4 and 5, taken for the same time period, are  
557 built of the different number of sectors. ICO aims to reduce overloads in configurations, so it uses the  
558 maximum number of controlled sectors per configuration. In the existing configurations, the number of  
559 sectors can vary depending on the number of available controllers during the day. Then, our algorithm  
560 tries to find configurations with the most suitable number of sectors. This means that the number of  
561 sectors in configuration created by the algorithm roughly derives from the chosen value of the targeted  
562 workload and the total workload of the ACC for the given time period.

563 Presented results show that our method, which freely combines airspace blocks, enables to  
564 propose balanced sectors configuration. The algorithm attempts to keep the value of the workload of  
565 each controlled sector close to some given value. The quality of the workload balance is linked to the  
566 performance of the algorithm and to the features of the benchmark. Indeed, if there are many input  
567 blocks almost equally loaded, it is easy to find a well balanced solution (Table 3). Considered here  
568 Maastricht ACC is originally divided into non-equally loaded airspace blocks, which are evidently hard to  
569 group into several equally loaded controlled sectors. Airspace blocks used for the second scenario  
570 increase the adaptability of the airspace to the traffic pattern, however shapes of these blocks are not  
571 enough convex. As a result, controlled sectors in the second scenario are better balanced, but show  
572 less performance in terms of other costs. If we want to obtain rather balanced sectors with good shapes  
573 and better adapted to the traffic, a new set of initial blocks is required.

## 574 **7 Conclusions**

575 The algorithm presented in this paper solves the DAC problem. At the first step, a weighted graph of the  
576 airspace has been proposed. Based on this initial graph, a method for solving a multi-period graph  
577 partitioning problem has been developed. Due to the induced complexity, a population-based  
578 metaheuristic optimization algorithm has been chosen for solving the DAC problem.

579 Genetic algorithms give good results on graph partitioning problems, but at some computational  
580 cost. The number of criteria and constraints in the DAC problem is highly increasing the complexity of  
581 the algorithm. One of the main problems for us was to create suitable recombination operators, which  
582 could sufficiently enrich the space of solutions.

583           The developed algorithm, applied to real airspace, has produced realistic and fairly good results.  
584 Computed configurations have been compared with the existing airspace configurations and with  
585 results obtained using ICO tool, developed by Eurocontrol. The provided results demonstrate that the  
586 new solution fits with the requirements of the DAC concept and in some way outperforms the existing  
587 ones.

588           Further improvements can be investigated to improve the performance of the algorithm. We can  
589 use more advanced workload metric in order to better reflect the associated traffic complexity in the  
590 sector. For instance, we could use a metric like convergence rate or Lyapunov exponents (Delahaye  
591 and Puechmorel, 2010). Then, in order to obtain operationally feasible sectors, it would require adding  
592 more geometrical constraints.

593

## 594 **References**

595 Antosiewicz, M., Koloch, G., Kaminski, B., 2013. Choice of best possible metaheuristic algorithm for the  
596 travelling salesman problem with limited computational time: quality, uncertainty and speed.  
597 Journal of Theoretical and Applied Computer Science 7(1), 46-55.

598 Back, T., Hoffmeister, F., Schwefel, H., 1991. A survey of evolution strategies. In: The fourth  
599 International Conference on Genetic Algorithm, San Mateo, 1991.

600 Bloem, M., Gupta, P., 2010. Configuring airspace sectors with approximate dynamic programming. In:  
601 The 27th International Congress of the Aeronautical Sciences (ICAS), Nice, 2010.

602 Blum, C., Roli, A., 2003. Metaheuristics in combinatorial optimization: overview and conceptual  
603 comparison. ACM Computing Surveys 35 (3), 268-308.

604 Christien, R., Benkouar, A., Chaboud, T., et al., 2003. Air traffic complexity indicators and ATC sectors  
605 classification. In: 21st Digital Avionics Systems Conference, Irvine, 2003.

606 Davis, L., 1991. Handbook of Genetic Algorithms. Van Nostrand Reinhold, New York.

607 Delahaye, D., Alliot, J., Schoenauer, M., et al., 1995. Genetic algorithms for automatic regrouping of air  
608 traffic control sectors. In: The 4th International Conference on Evolutionary Programming, San



609           Diego, 1995.

610 Delahaye, D., Puechmorel, S., 2010. Air traffic complexity based on dynamical systems. In: The 49th  
611           IEEE Conference on Decision and Control, Atlanta, 2010.

612 Delahaye, D., Schoenauer, M., Alliot, J.M., 1998. Airspace sectoring by evolutionary computation. In:  
613           The IEEE World Congress on Computational Intelligence, Anchorage, 1998.

614 Eurocontrol, 2015. Dynamic airspace configuration. Technical report, SESAR WP7.5.4 project, OSED  
615           step2/V2.

616 Fogel, L., Owens, A., 1966. Artificial Intelligence Through Simulated Evolution. John Wiley & Sons,  
617           London.

618 Gianazza, D., 2010. Forecasting workload and airspace configuration with neural networks and tree  
619           search methods. Artificial Intelligence 174(7-8), 530-549.

620 Goldberg, D., 1989. Genetic Algorithms in Search, Optimization and Machine Learning, first ed.  
621           Addison-Wesley Longman Publishing Co., Inc., Boston.

622 Han, S.C., Zhang, M., 2004. The optimization method of the sector partition based on metamorphic  
623           voronoi polygon. Chinese Journal of Aeronautics 17(1), 7-12.

624 Holland, J., 1975. Adaptation in Natural and Artificial Systems. Massachusetts Institute of Technology  
625           (MIT) Press, Cambridge.

626 Kernighan, B.W., Lin, S., 1970. An efficient heuristic procedure for partitioning graphs. The Bell System  
627           Technical Journal 49 (2), 291-307.

628 Klein, A., Lucic, P., Rodgers, M., et al., 2012. Exploring tactical interaction between dynamic airspace  
629           configuration and traffic flow management (DAC-TFM). In: The 31st Digital Avionics Systems  
630           Conference, Williamsburg, 2012.

631 Klein, A., Rodgers, M., Kaing, H., 2008. Dynamic FPAs: a new method for dynamic airspace  
632           configuration. In: Integrated Communications, Navigation and Surveillance Conference,  
633           Bethesda, 2008.

634 Kohonen, J., 1999. A brief comparison of simulated annealing and genetic algorithm approaches.  
635           Available at: <https://www.cs.helsinki.fi/u/kohonen/papers/gasa.html> (Accessed 1 April 2016).

636 Kopardekar, P., Bilimoria, K., Banavar, S., 2007. Initial concepts for dynamic airspace configuration. In:  
637 The 7th American Institute of Aeronautics and Astronautics (AIAA) Aviation Technology,  
638 Integration and Operation Conference (ATIO) Conference, Atlanta, 2007.

639 Koza, J., 1992. Genetic Programming. MIT Press, Cambridge.

640 Majumdar, A., Ochieng, W., 2002. Factors affecting air traffic controller workload: multivariate analysis  
641 based on simulation modelling of controller workload. Transportation Research Record 1788,  
642 58–69.

643 Martinez, S., Chatterji, G., Sun, D., et al., 2007. A weighted-graph approach for dynamic airspace  
644 configuration. In: The AIAA Conference on Guidance, Navigation, and Control (GNC), Atlanta,  
645 2007.

646 Michalewicz, Z., 1992. Genetic algorithms + Data Structures = Evolution Programs. Springer-Verlag,  
647 Berlin.

648 Miller, B.L., Goldberg, D.E., et al., 1995. Genetic algorithms, tournament selection, and the effects of  
649 noise. Complex Systems 9(3), 193–212.

650 Mukherjee, S., Datta, S., Chanda, P.B., et al., 2015. Comparative study of different algorithms to solve  
651 n-queens problem. International Journal in Foundations of Computer Science and Technology  
652 (IJFCST) 5(2), 15-27.

653 Nair, T.R.G., Sooda, K., 2010. Comparison of Genetic Algorithm and Simulated Annealing Technique  
654 for Optimal Path Selection in Network Routing. arXiv: 1001.3920. Available at:  
655 <http://arxiv.org/abs/1001.3920> (Accessed 1 April 2016).

656 Rossi-Doria, O., Sampels, M., Birattari, M., et al., 2002. A Comparison of the Performance of Different  
657 Metaheuristics on the Timetabling Problem. In: International Conference on the Practice and  
658 Theory of Automated Timetabling, Berlin, 2002.

659 Savage, J.E., Wloka, M.G., 1989. Heuristics for Parallel Graph-partitioning. Brown University,  
660 Providence.

661 Sergeeva, M., Delahaye, D., Zerrouki, L., et al., 2015. Dynamic airspace configurations generated by  
662 evolutionary algorithms. In: The 34th Digital Avionics Systems Conference, Prague, 2015.

663 Silberholz, J., Golden, B., 2010. Comparison of metaheuristics, in: Gendreau, M., Potvin, J. (Eds.),

664 Handbook of Metaheuristics Springer-Verlag, Boston, pp. 625-640.

665 Talbi, E.G., 2009. Metaheuristics: from Design to Implementation. John Wiley & Sons, London.

666 Tang, J., Alam, S., Lokan, C., et al., 2011. A multi-objective approach for dynamic airspace sectorization  
667 using agent based and geometric models. Transportation Research Part C: Emerging  
668 Technologies 21(1), 89-121.

669 Trandac, H., Duong, V., 2002. A constraint-programming formulation for dynamic airspace sectorization.  
670 In: The 21st Digital Avionics Systems Conference, Irvine, 2002.

671 Vehlac, C.S.M., 2005. Improved configuration optimizer. ECC note No 10/05.

672 Chen, Y., Bi, H., Zhang, D., et al., 2013. Dynamic airspace sectorization via improved genetic algorithm.  
673 Journal of Modern Transportation 21(2), 117–124.

674 Zelinski, S., Lai, C.F., 2011. Comparing methods for dynamic airspace configuration. In: The 30th Digital  
675 Avionics Systems Conference, Seattle, 2011.

676

677

678

679

680

681

682

683

684

685

686

687

688

689

690

691



692

693 **Marina Sergeeva** received the MSc degree in computer science from Department of Information  
694 Measuring Systems and Physical Electronics at Petrozavodsk State University in 2010. She is currently  
695 working toward the PhD degree at Ecole Nationale de l'Aviation Civile (ENAC), Toulouse, France. Her  
696 research concerns airspace design.

697



698

699 **Daniel Delahaye** obtained his engineer degree from ENAC and his MSc in signal processing from the  
700 National Polytechnic Institute of Toulouse (1991). He obtained his PhD in automatic control from the  
701 Aeronautic and Space National School (1995). He is now the head of the optimization group of the  
702 MAIAA laboratory of ENAC and is conducting research on stochastic optimization for airspace design  
703 and large-scale traffic assignment.

704



705

706 **Catherine Mancel** received the MSc degree in computer science and production management from  
707 University of Clermont-Ferrand, France, in 2000, and the PhD degree in operations research from the  
708 National Institute of Applied Science (INSA), Toulouse, France in 2004. She is an associate professor  
709 with the ENAC, Toulouse, France, since 2005. She teaches and conducts research in air transportation

710 modelling and operations research.

711

712



713

714 **Andrija Vidosavljevic** graduated from the Faculty of Transport and Traffic Engineering, University of  
715 Belgrade (UB-FTTE) in 2007 in the field of air transportation. He received a PhD at the division of  
716 airports and air traffic safety from UB-FTTE in 2014. He is currently post-doctoral researcher at  
717 ENAC/MAIAA lab.

718